Received: 10 May 2023 | Revised: 3 November 2023 | Accepted: 7 November 2023

DOI: 10.1002/hbm.26539

RESEARCH ARTICLE

WILEY

# Decreased long-range temporal correlations in the resting-state functional magnetic resonance imaging blood-oxygen-level-dependent signal reflect motor sequence learning up to 2 weeks following training

Anna-Thekla P. Jäger[1,2,3] | Alexander Bailey[4] | Julia M. Huntenburg[1,5] | Christine L. Tardif[6,7] | Arno Villringer[1,2,8,9,10] | Claudine J. Gauthier[11,12] | Vadim Nikulin[1] | Pierre-Louis Bazin[1,13] | Christopher J. Steele[1,14]

[1]Department of Neurology, Max Planck Institute for Human Cognitive and Brain Sciences, Leipzig, Germany

[2]Center for Stroke Research Berlin (CSB), Charité—Universitätsmedizin Berlin, Berlin, Germany

[3]Brain Language Lab, Freie Universität Berlin, Berlin, Germany

[4]Temerty Faculty of Medicine, University of Toronto, Toronto, Ontario, Canada

[5]Max Planck Institute for Biological Cybernetics, Tuebingen, Germany

[6]Department of Biomedical Engineering, McGill University, Montreal, Québec, Canada

[7]Montreal Neurological Institute, Montreal, Québec, Canada

[8]Clinic for Cognitive Neurology, Leipzig, Germany

[9]Leipzig University Medical Centre, IFB Adiposity Diseases, Leipzig, Germany

[10]Collaborative Research Centre 1052-A5, University of Leipzig, Leipzig, Germany

[11]Department of Physics/School of Health, Concordia University, Montreal, Québec, Canada

[12]Montreal Heart Institute, Montreal, Québec, Canada

[13]Faculty of Social and Behavioral Sciences, University of Amsterdam, Amsterdam, Netherlands

[14]Department of Psychology/School of Health, Concordia University, Montreal, Québec, Canada

**Correspondence**
Christopher J. Steele, Department of Neurology, Max Planck Institute for Human Cognitive and Brain Sciences, Leipzig 04103, Germany.
Email: christopher.steele@concordia.ca

**Funding information**
Fonds Recherche Québécois Nature et Technologies; Heart and Stroke Foundation of Canada; MaxNetAging Research School; Michal and Renata Hornstein Chair in Cardiovascular Imaging; National Science and Engineering Research Council, Grant/Award Numbers: RGPIN 2015-04665, RGPIN-2020-06812; NWO Vici grant

## Abstract

Decreased long-range temporal correlations (LRTC) in brain signals can be used to measure cognitive effort during task execution. Here, we examined how learning a motor sequence affects long-range temporal memory within resting-state functional magnetic resonance imaging signal. Using the Hurst exponent (HE), we estimated voxel-wise LRTC and assessed changes over 5 consecutive days of training, followed by a retention scan 12 days later. The experimental group learned a complex visuo-motor sequence while a complementary control group performed tightly matched movements. An interaction analysis revealed that HE decreases were specific to the complex sequence and occurred in well-known motor sequence learning associated regions including left supplementary motor area, left premotor cortex, left M1, left

Pierre-Louis Bazin and Christopher J. Steele contributed equally to this work.

pars opercularis, bilateral thalamus, and right striatum. Five regions exhibited moderate to strong negative correlations with overall behavioral performance improvements. Following learning, HE values returned to pretraining levels in some regions, whereas in others, they remained decreased even 2 weeks after training. Our study presents new evidence of HE's possible relevance for functional plasticity during the resting-state and suggests that a cortical subset of sequence-specific regions may continue to represent a functional signature of learning reflected in decreased long-range temporal dependence after a period of inactivity.

**KEYWORDS**
Hurst Exponent, Learning, long-range temporal correlations, Motor Sequence Learning, Plasticity, resting-state, self-similarity

## 1 | INTRODUCTION

Brain activity from blood oxygenation level dependent (BOLD) functional magnetic resonance imaging (fMRI) data has been shown to exhibit long-range temporal correlations (LRTC) indicating self-similar properties—a phenomenon whereby small components of a complex system share the same structure and behavior as their larger counterparts (see Campbell & Weber, 2022, for a comprehensive review).

A growing body of research in fMRI and electroencephalography (Barnes et al., 2009; Churchill et al., 2014; Churchill et al., 2016; Colosio et al., 2017; He, 2011; Irrmischer et al., 2018; Wink et al., 2006) has shown that more effortful/stressful conditions exhibit greater reductions in long-range temporal dependence during tasks. Based on this work, the "suppression" of signal self-similarity has been proposed as a generalizable neuroimaging marker for neuronal recruitment or higher cognitive effort (Kardan et al., 2020). Interestingly, higher temporal signal variability—which itself is reflected in lower self-similarity—has been linked to greater brain efficiency and cognitive flexibility (McIntosh et al., 2010; Tognoli & Scott Kelso, 2014). Due to its relevance in demanding conditions and its association with cognitive effort, brain efficiency, and cognitive flexibility, the Hurst exponent (HE) holds promise for studying learning and neuroplasticity. This raises the question: Are neuroplastic processes reflected by the long-range temporal memory in task-related brain regions following skill learning?

Previous studies have demonstrated that increasing external input to the brain, such as through eyes-open versus eyes-closed conditions (Nikulin & Brismar, 2004) or median nerve stimulation (Linkenkaer-Hansen et al., 2004), leads to temporary transient decreases in LRTC as measured by the HE. Similarly, Barnes et al. (2009) observed lower LRTC during cognitive performance that was followed by recovery to baseline levels ~15 min after completing the task. These and similar studies have proposed that there are baseline levels of self-similarity that are temporarily disturbed by active tasks /cognitive effort (Barnes et al., 2009; Churchill et al., 2016; Tetereva et al., 2020; Wenger et al., 2017). Other studies have reported that increased LRTC in resting state data is reflective of prior task performance (Mahjoory et al., 2019; Samek et al., 2016; Wink et al., 2006). In addition, baseline self-similarity levels have also been shown to be altered in clinical populations and as an effect of aging (Dong et al., 2018; Maxim et al., 2005; Sokunbi et al., 2014; Suckling et al., 2008; Wei et al., 2013; Wink et al., 2006) providing further evidence that they are subject to change. Finally, recent research has shown that LRTC's at rest in cortical areas are at least partially explained by the eigenvector centrality (EC) of the connected white matter (Neudorf et al., 2020), supporting the idea that structural changes may also be paralleled by changes in long-range temporal dependence. Here, we sought to investigate directly how and whether self-similar baseline levels at rest would be affected by an ongoing active learning period and if so, whether changes in LRTC's properties would return to pretraining levels after some time without training.

In our recent study (Jäger et al., 2022), we explored functional neuroplasticity following sequence-specific motor sequence learning (MSL) using time series cross-correlations and graph network-based analysis with EC mapping and found a prominent role for the supplementary motor area (SMA). The current study builds upon this work to establish the utility and efficacy of HE as a potential new indicator of identifying functional neuroplasticity in response to MSL. Given that HE is computed on a single region/voxel's time series, and that fluctuations in the time series signal are a function of activity in connected regions, we hypothesize that HE changes across learning will reflect altered training-related connectivity and information processing in the brain. The longitudinal design of our experiment also gave us the opportunity to investigate the progression of long-range temporal dependence in rs-fMRI over time.

## 2 | METHODS

As a brief overview, twenty participants were trained on a complex visuomotor pinch-force MSL task (Gryga et al., 2012) and matched to a nonlearning control group to precisely identify task-specific changes in self-similarity. The task was trained on 5 consecutive days (~12 min per day), with two additional sessions: one familiarization session

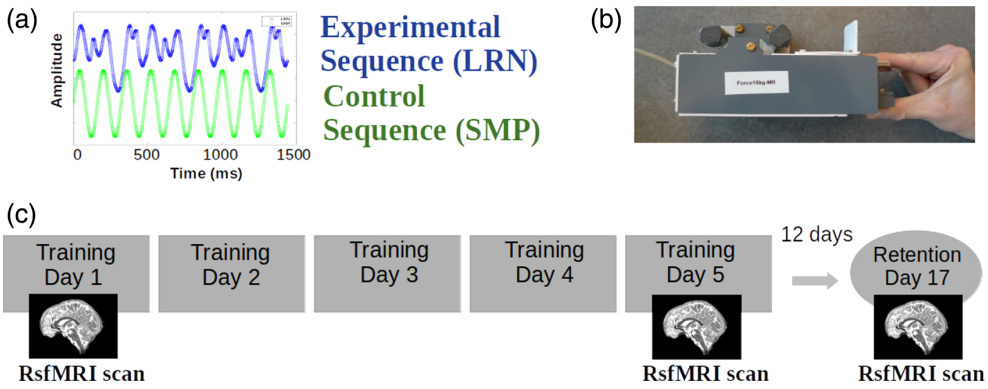


**FIGURE 1** (a) The two sequences: LRN (blue) & SMP (green), (b) the pinch force device, and (c) the general procedure and study design. Behavioral training took place on 5 consecutive days and again 12 days later, whereas rsfMRI data were collected on d1, d5, and d17.

3 days prior and one retention session after the training period (12 days later). We assessed scale-free dynamics with the HE estimated from detrended fluctuation analysis (DFA), a mathematical method used to investigate the presence of long-range correlations, or fractal-like patterns, in time series data (for a more detailed description see the section "Detrended Fluctuation Analysis"). Whole brain HE maps were computed before (on day 1) and after learning the task (on day 5) as well as 12 days after no additional training took place. The present data has been published in previous studies, which focused on measures of functional connectivity and white matter changes, respectively (Jäger et al., 2022; Tremblay et al., 2021). The majority of the methods have previously been described in detail in (Jäger et al., 2022) and will briefly be presented here.

### 2.1 | Participants

Participants were recruited at the Max Planck Institute for Human Cognitive and Brain Sciences (Leipzig, Germany) and the study design was approved by the Leipzig University ethics review board. The sample size was 40 (22 females, right-handed) with 20 participants (11 females) being randomly assigned to the experimental group and 20 (10 females) to the control group (age range = 20–32). While the experimental group learned a complex visuomotor sequence (first presented in Gryga et al., 2012, see Figure 1a), the control group executed a simple sinusoidal sequence matched for motor execution. The experimental design consisted of a familiarization session, 5 consecutive days of training, and a retention session after 12 days, see Figure 1c.

## 3 | EXPERIMENTAL DESIGN

### 3.1 | Task and stimuli: Sequential pinch force task

Participants used their index fingers and thumb to generate a pinching force onto a device that measured force 80 times per second. On a screen, participants were presented with a rectangular yellow force bar (FOR) representing the pinching force. Movement of the bar (height of the bar over time) was controlled by pinching the device (see Figure 1b)—where stronger force led to greater height of the bar. The level of force was set to 5%–30% of each participant's measured maximum force (measured at the start of the first session) to match relative effort across participants. Participants were instructed to match the height of the FOR bar to the height of an adjacent blue rectangular reference (REF) bar that moved up and down according to a preprogrammed sequence by pinching the device accordingly. The movement of REF was controlled under three different conditions: learning (LRN: complex sequence, REF bar moves according to a complex pattern), simple control (SMP: simple sequence, REF moves up and down in a sinusoidal manner), and rest (RST: resting condition, no moving bars) (Gryga et al., 2012). SMP was matched to LRN for the total magnitude of force, frequency of maximum power, duration, and range of force. Therefore, both groups executed the same type of movements by varying pinch force over time but differed in the extent of learning required to accurately perform the sequence. Consequently, the behavioral improvement during LRN provides information about sequence-specific learning when contrasted with SMP. During training, each condition was administered for 18 s per trial and structured into blocks, where one block consisted of three LRN, SMP, and RST trials. For each training day, the LRN group performed three blocks (nine trials), whereas the SMP group performed the same amount of blocks without the LRN condition (LRN was replaced by SMP). Participants received feedback on their performance in terms of average accuracy in matching the heights of the FOR and REF bars in the LRN and SMP condition at the end of each block.

### 3.2 | Training and experimental procedure

MSL trials consisted of participants performing the sequential pinch force task (SPFT) during five training sessions (d1–d5) preceded by a familiarization session (d0) and followed after 12 days by a retention session (d17). The measurements took place inside the MRI scanner on five of the seven training days (d0, d1, d2, d5, and d17), whereas two sessions took place inside a testing room outside of the scanner (d3 and d4). We included three of these MRI measurements in the current analyses (d1, d5, and d17) representing the overall learning period as well as retention (Jäger et al., 2022). We chose those three timepoints because the behavioral analysis and our previous results

demonstrated an accurate representation of performance improvements representative of learning the task between d1 and d5 and because we were further interested in the temporal dynamics of learning-related self-similarity following the training period.

### 3.3 | Scanning protocol

MRI scans were conducted using a 7 Tesla MAGNETOM scanner from Siemens Healthcare situated at the Max Planck Institute for Human Cognitive and Brain Sciences in Leipzig, Germany with a 32-channel Nova head coil was also utilized. RsfMRI scans comprised of echo planar imaging (EPI) BOLD with 1.2 × 1.2 × 1.2 mm resolution, 512 volumes, field of view (FOV) = 192 × 192 $mm^2$, slice acceleration factor: 2 and 102 slices; generalized autocalibrating partial parallel acquisition (GRAPPA) = 2 and partial Fourier 6/8; repetition time (TR) = 1130 ms; echo (TE) = 22 ms; flip angle = 40° and bandwidth 1562 Hz/Px. They were acquired over 10 min while participants kept their eyes open and attended to a fixation cross approximately 20 min prior to acquiring the task-based fMRI data. Additionally MP2RAGE images had 0.7 × 0.7 × 0.7 mm resolution, with an FOV = 224 × 224 × 240 $mm^3$, 240 slices; TR = 5000 ms; TE = 2.45 ms; flip angle 1 = 5°, flip angle 2 = 3°, bandwidth 250 Hz/Px. Fieldmaps had a 2 × 2 × 2 mm resolution with an FOV 256 × 256 $mm^2$ having 80 slices; TR 18 ms; TE1 4.08 ms;TE2 918 ms; flip angle 10° bandwidth 300 Hz/Px.

### 3.4 | Image processing

Preprocessing of functional images was implemented using Nipype (Gorgolewski et al., 2016) and Nilearn (v0.2.3, Abraham et al., 2014; Pedregosa et al., 2011). The first five volumes of the rsfMRI EPI sequence were removed and the remaining images underwent motion correction (Roche, 2011) as well as fieldmap correction with FUGUE (Jenkinson, 2004; Jenkinson et al., 2012). Average brain signal and motion-related outliers were removed through ArtifactDetect alongside white matter and cerebrospinal fluid signals (high_variance_confounds/Nilearn). Afterward, the time series' variance was normalized, bandpass filtered between 0.01 and 0.1 Hz and smoothed with a 3.6 mm Gaussian kernel (Poldrack et al., 2011) before DFA computation for HE maps generation in native space. To bring these maps into montreal neurological institute (MNI) space for group analysis, Jäger et al.'s (2022) longitudinal co-registration pipeline were used, which included 12 d of linear transformation nonlinear SYN transformations conducted with advanced normalization tools (Avants et al., 2009) and implemented with the CBS Tools (Bazin et al., 2014). Intermediate procedures such as tissue segmentation, masking, or generating transformation maps between native/group/MNI spaces were also conducted with CBS Tools. All scripts related to this preprocessing are available at https://github.com/AthSchmidt/MMPI/tree/master/preprocessing.

### 3.5 | Detrended fluctuation analysis

DFA is a commonly used method to study self-similarity based on analyzing the temporal autocorrelation of time series (Hardstone et al., 2012). It calculates the HE, a robust estimate of the degree of self-similarity of a temporal signal (Churchill et al., 2016; Eke et al., 2012; He, 2011). For brain imaging data, DFA provides a univariate representation of each region's intrinsic time-varying dynamic activity, with higher HE indicating highly temporally autocorrelated signals (greater LRTC), and lower HE indicating lower temporal autocorrelation (lower LRTC, often interpreted as greater complexity and variability). Specifically, for time series data, HE reflects the slope (i.e., least squares fit) of the log–log relationship between the time window size and the mean variance of linearly detrended cumulative signal measured in windows of different sizes (Hardstone et al., 2012; Schaworonkow et al., 2015). In this study, we computed HE using 15 log-spaced windows ranging from a minimum of 10 samples to a maximum of 57, corresponding to the following number of samples in each windowing step: 10, 11, 12, 14, 16, 18, 20, 23, 26, 28, 32, 39, 43, 47, and 57. HE values in the range of 0.5–1 reflect persistent long-range dependencies increasing toward 1, whereas 0.5 reflects a random (white noise) uncorrelated process (Campbell & Weber, 2022; Hardstone et al., 2012).

## 4 | STATISTICAL ANALYSIS

### 4.1 | Baseline HE changes prior to training

We first set out to confirm that baseline HE maps between the two groups did not differ before the training period by conducting independent *t*-tests on d0 and d1 (d0: LRN vs. SMP; d1: LRN vs. SMP) with SPM (Friston et al., 1994). All whole brain analyses were assessed for significance using cluster correction (primary cluster-forming threshold = $p < .001$) and false discovery rate (fdr) correction ($p < .05$) (Woo et al., 2014).

### 4.2 | Behavioral analysis

The results of the behavioral data analysis conducted in two earlier studies (Jäger et al., 2022; Tremblay et al., 2021) were used for visualization (Figure 2) and to determine which timepoints should be correlated with behavior. Further details can be found in those prior studies.

### 4.3 | Sequence-specific learning

To conduct the interaction analysis, a flexible factorial design for longitudinal data from the CAT12 toolbox (http://www.neuro.uni-jena.de/cat/) was used. The design included two factors, group (LRN/SMP)

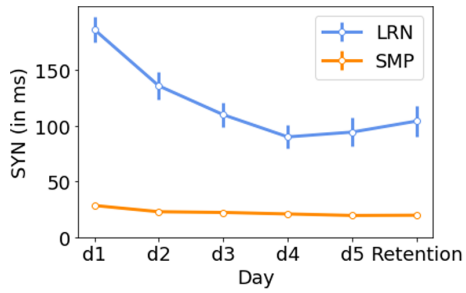


**FIGURE 2** The temporal synchronization (SYN, in ms) results for both groups (LRN and SMP) across all days (d1–d17). Error bars reflect the standard error of the mean, with LRN values calculated by averaging 3 trials × 3 blocks per day and SMP values obtained from averaging 6 trials × 3 blocks per day.

and time (d1 and d5), and we conducted separate analyses to identify both increases and decreases across time. Subsequently, to understand which group was driving the effect, the magnitudes of HE changes were calculated within any significant region of interest (ROI) and compared between groups. Consistent with our previous work (Jäger et al., 2022), we defined sequence-specific change as any significant interaction where change was greater in the LRN group than it was in the SMP group.

### 4.4 | Quality control—Impact of motion on results

Framewise displacement (FD) was computed to assess the potential influence of in-scanner motion on the results. Mean FD (meanFD) was separately calculated for d1 and d5 (the sessions of interest) in each participant of the learning group. The absolute translational displacement was calculated by finding the absolute differences in the translation parameters between consecutive time points, representing the subject's movement in the x, y, and z directions. Absolute rotational displacement was calculated similarly, by determining the absolute differences in the rotation parameters between consecutive time points, with a conversion from radians to millimeters. The absolute translational and rotational displacements were combined to derive the absolute FD for each time point. Finally, the mean FD was obtained as the average of all absolute FD values across all time points (Power et al., 2012). MeanFD value changes between d1 and d5 were then correlated with the corresponding HE changes from all significant clusters obtained in the initial interaction analysis and corrected for multiple comparisons.

### 4.5 | Correlations with behavioural improvement

Significant clusters from the interaction analysis were considered ROIs that constitute the sequence-specific learning network. To test whether the change in HE in those regions was related to behavioral improvement, we correlated (using Pearson's coefficient) the overall performance improvements with values from the identified sequence-specific learning network. In our previous study, we found that learning plateaued on d4 of the training period (Figure 2), providing evidence that the overall behavioral learning period took place between d1 and d4. Therefore we operationalized overall learning as the difference between the last block of d4 and the first block of d1 (d4b3-d1b1) on temporal synchronization (SYN). Considering that MR data was not collected on d4 and that on scanning days the rsfMRI acquisition was collected before task performance, we chose d5 as the most appropriate measurement to represent the brain's functional state at this time point. The mean difference (d5–d1) was calculated for each ROI in each participant and then correlated with the performance improvement in SYN using pearsonr from Scipy (Virtanen et al., 2020).

Additional correlation analyses were conducted to test whether HE values before, during, and after learning were correlated with behavioral improvements (Mahjoory et al., 2019; Samek et al., 2016; Wink et al., 2006) to identify potential behavioral relevance. For these analyses, we correlated mean HE within each ROI on d1, d5, and d17 with the previously calculated behavioral improvement (SYN d4b3-d1b1). The resulting correlations were corrected with fdr correction for multiple comparisons using the *p*.adjust function in R (R Core Team, 2021). Visualizations were created in Python with seaborn (Waskom, 2021) and matplotlib (Hunter, 2007).

### 4.6 | Maintenance versus recovery at posttraining retention

Finally, to examine the HE trajectories after training, namely whether HE would return to baseline levels (Barnes et al., 2009) or stay altered after 2 weeks without training, ROI mean values were extracted from all significant clusters previously found in the interaction analysis and single sample paired *t*-tests were conducted between d1/d17 and d5/d17 within the LRN group. When there was a significant difference between d1 and d17 but not d5 and d17, clusters were categorized as showing no recovery to baseline. When there was no significant difference between d1 and d17 but there was between d5 and d17, ROIs were categorized as returning to baseline. For validation purposes, we also further explored the retention period with an interaction analysis and have included these results in Supplementary Figure S2.

## 5 | RESULTS

### 5.1 | Baseline HE changes prior to training and the potential effects of motion

There were no significant differences in HE between groups before training on either d0 (all $p$[fdr] > .673, $k$ < 86) or d1 (all $p$[fdr] > .184, all $k$ < 63). There was also no significant correlation between meanFD changes between d1 and d5 and HE changes between d1 and d5 (all $p$ [bonferroni] > 0.47).

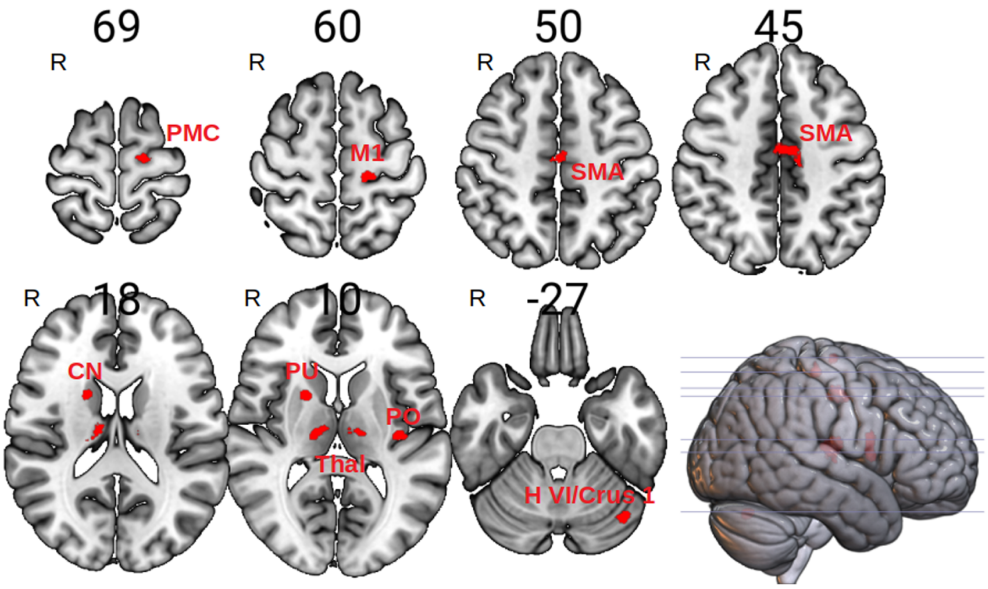


**FIGURE 3** Interaction effects: Decreases in HE in the LRN group between d1 and d5 in the left SMA (slices 50 and 45), left premotor cortex (slice 69), left M1 (slice 60), left PO, bilateral thalamus and right striatum (slice 10) as well as left lobule H VI/Crus I (slice 27).

**TABLE 1** Summary statistics for clusters exhibiting significant time-by-group interactions. Mean differences between d1 and d5 and the standard error of the mean difference are shown. Sequence-specific regions (where LRN exhibited greater change than SMP, top) and regions that were not to be found sequence-specific (bottom) are grouped together.

| | | LRN | | | SMP | | |
|---|---|---|---|---|---|---|---|
| **Region** | **MNI coordinates** | **Mean change** | **SEM** | **95% CI** | **Mean change** | **SEM** | **95% CI** |
| Sequence-specific clusters | | | | | | | |
| L SMA | −14 −13 43 | −0.1 | 0.02 | −0.15 to −0.06 | 0.03 | 0.02 | −0.01 to 0.07 |
| L PO | −35 −18 13 | −0.1 | 0.03 | −0.14 to −0.04 | 0.04 | 0.03 | −0.01 to 0.09 |
| R thalamus | 13 −17 17 | −0.07 | 0.02 | −0.11 to −0.03 | 0.05 | 0.03 | 0.004 to 0.11 |
| L thalamus | −8 −14 14 | −0.07 | 0.02 | −0.12 to −0.03 | 0.05 | 0.03 | −0.01 to 0.11 |
| L M1 | −17 −14 68 | −0.09 | 0.03 | −0.14 to −0.04 | 0.04 | 0.03 | −0.02 to 0.09 |
| L premotor cortex | −18 −26 61 | −0.08 | 0.02 | −0.14 to −0.03 | 0.04 | 0.03 | −0.02 to 0.1 |
| Clusters not showing sequence-specificity | | | | | | | |
| R striatum | 20 8 8 | −0.06 | 0.02 | −0.09 to −0.02 | 0.07 | 0.02 | 0.03 to 0.11 |
| L H VI/Crus I | −41 −70 −26 | −0.06 | 0.01 | −0.09 to −0.03 | 0.07 | 0.03 | 0.01 to 0.13 |

*Note*: Mean differences between d1 and d5 and the standard error of the mean difference are shown. Sequence-specific regions (where LRN exhibited greater change than SMP, top) and regions that were not to be found sequence-specific (bottom) are grouped together.

### 5.2 | Sequence-specific learning

Significant between-group interaction effects from d1 (prior to active training) to d5 (after active training) were found in the left SMA & pars opercularis (PO), left premotor cortex, left primary motor cortex (M1), bilateral thalamus, right striatum (with a cluster covering the caudate nucleus and putamen), and left cerebellar lobule H VI/ Crus I (Figure 3). In all cases, HE values decreased over the course of learning in the LRN group while they exhibited mean increases in the SMP group. HE trajectories over the course of the experiment for both groups in all significant ROIs can be found in the supplementary materials (Figure S1). Sequence-specific learning effects (i.e., where LRN elicited a greater change in HE during learning compared to SMP) were found in all clusters except the Striatum and lobule H VI/Crus I (Table 1, all $p < .05$).

### 5.3 | Correlations with behavioural improvement

There were no significant findings from the initial correlation analyses between ROI HE difference values (d5–d1) and performance improvement (d4–d1) (all fdr corrected: L SMA: $p > .42$; L PMC: $p > .86$; L M1: $p > .88$; L PO: $p > .30$; R thalamus: $p > .63$; L thalamus: $p > .42$; R S: $p > .24$, L H VI/Crus I: $p > .86$). However, the subsequent exploratory correlation analysis between mean HE from sequence-specific learning clusters (R & L thalamus, R striatum, L SMA & PO) on d5 and the observed behavioral overall performance improvements in SYN between between d1 (Block1) and d4 (Block3) d1 and d4 (reflecting overall performance improvements before data acquisition on d5) showed significant associations in several of the regions (Figure 4). Improvements in behavioral performance were negatively correlated with HE on d5 in the left SMA (all $p$'s fdr corrected: $r = 0.63$, $p = .01$),

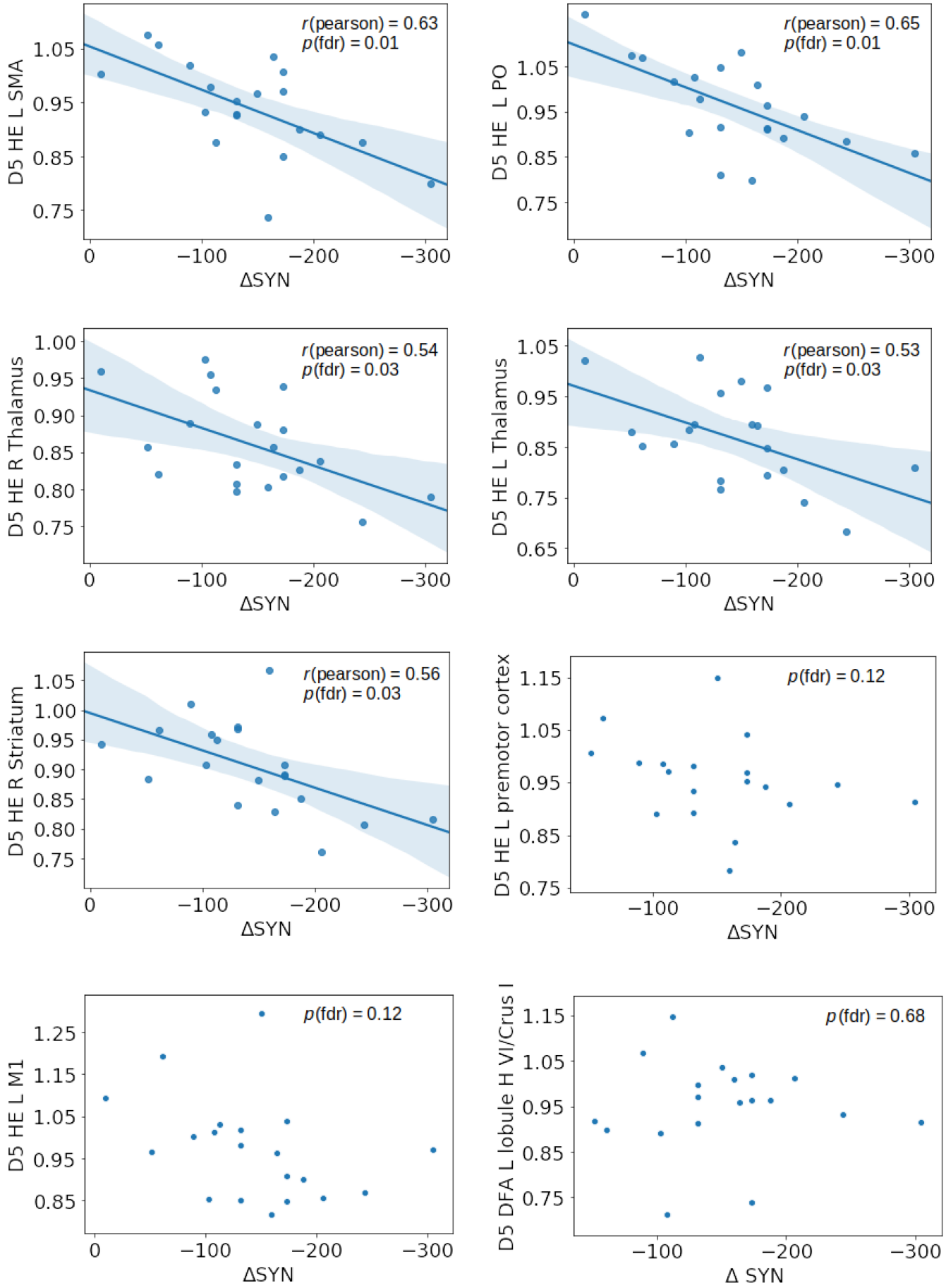


**FIGURE 4** Legend on next page.

left PO ($r = 0.65$, $p = .01$), right thalamus ($r = 0.54$, $p = .03$), left thalamus ($r = 0.53$, $p = .03$) and right striatum ($r = 0.56$, $p = .03$) indicating that lower self-similarity of the rsfMRI signal following learning was reflective of higher overall performance improvements.

When investigating the predictive qualities of HE for overall improvement, further exploratory correlational analyses between HE on d1 with behavioral improvement did not yield significant results (all $p$[fdr] > .623). When investigating whether the maintained decreases after 2 weeks also correlated with the overall behavioral improvements, we also found no significant relationships (all $p$[fdr] > .74).

### 5.4 | Maintenance versus recovery at posttraining retention

Further investigations of recovery of HE following training showed region-specific effects. Post hoc tests (d1–d5, d5–d17, and d1–d17) confirmed significant HE differences between d1 and d5, as previously identified in the interaction analysis. In five regions including the left SMA, left M1, left premotor cortex, left PO, and left striatum, the paired sample $t$-tests showed a significant difference between d1 and d17 (SMA: $p = .0004$, M1: $p = .008$, premotor: $p = .015$, PO: $p = .011$, striatum: $p = .039$) but not d5 and d17 (all $p > .15$), suggesting no evidence for the recovery of HE to baseline levels and implying that the change between d1 and d5 persisted for at least 12 days without training (Figure 5). On the other hand, HE in the right thalamus was significantly different between d5 and d17 (right thalamus: $p = .048$) but not between d1 and d17 ($p > .2$), indicating an HE recovery towards pretraining levels after 12 days without training. Finally, d17 HE in the left thalamus and left lobule H VI/Crus I was neither significantly different from d1 or d5 (all $p > .09$).

## 6 | DISCUSSION

This study investigated how changes in LRTC in the rsfMRI BOLD signal reflect ongoing functional plasticity related to complex sequence learning. The identified regions displayed a decrease in LRTC, reflective of sequence-specific learning and performance improvements. Following a 2-week break from training, LRTC of most regions showing sequence-specific changes did not return to baseline, suggesting that training-induced specific alterations in functional dynamics may represent the newly learned skill. We conclude that decreased LRTC may present as a sensitive measure of neuroplastic change resulting from complex motor learning.

### 6.1 | HE is a relevant measure for studying MSL and plasticity

Our interaction analysis confirmed the involvement of regions often identified to show learning in the MSL literature (e.g., Bernard & Seidler, 2013; Dayan & Cohen, 2011; Hardwick et al., 2013; Janacsek et al., 2020; Kawai et al., 2015; Kornysheva & Diedrichsen, 2014; Krakauer et al., 2019; Lehéricy et al., 2005; Matsuzaka et al., 2007; Reithler et al., 2010; Steele & Penhune, 2010; Tanji & Shima, 1994); including the left SMA, M1, premotor cortex, PO, lobule H VI/Crus I of the cerebellum, bilateral thalamus and right striatum. These clusters were characterized by significant decreases in HE over the learning period from d1 to d5 for the experimental group in contrast to the control group. By specifying our results to those regions where the training group exhibited greater change than the control group (i.e., regions exhibiting sequence-specific plasticity), we identified a sequence-specific learning network including the SMA, M1, premotor cortex, left PO, and bilateral thalamus. The SMA, PO, thalamus, and striatum were also significantly correlated with behavioral performance improvements over the learning period. SMA and premotor cortex have repeatedly been linked to sequence-specific learning (Berlot et al., 2020; Elsinger et al., 2006; Gaymard et al., 1990; Gerloff et al., 1997; Grafton et al., 2002; Hardwick et al., 2013; Hikosaka et al., 1999; Honda et al., 1998; Jenkins et al., 1994; Kincses et al., 2008; Lee & Quessy, 2003; Mushiake et al., 1991; Penhune & Steele, 2012; Shibasaki et al., 1993; Shima & Tanji, 2000; Steele & Penhune, 2010; Tanaka et al., 2010; Vollmann et al., 2013; Wu et al., 2014; Yokoi & Diedrichsen, 2019). Yet, debates exist regarding the involvement of M1 (Floyer-Lea & Matthews, 2005; Kami et al., 1995; Karni et al., 1998; Kawai et al., 2015; Lehéricy et al., 2005; Penhune & Doyon, 2002; Picard et al., 2013; Wiestler & Diedrichsen, 2013; Yokoi et al., 2018). Our data suggests that M1 is involved as evidenced by a larger decrease in LRTC in learners as compared to the control group. However, activity within M1 and premotor cortex did not correlate with performance. It has been proposed that M1 may be most important for individual finger movements (Yokoi & Diedrichsen, 2019), which could explain our findings given LRN had a higher frequency of movements compared to SMP. Future studies should consider alternative sequences matching each other's movement frequencies to fully understand how M1 contributes to sequence-specific learning mechanisms. Taken together, our sequence-specific results combined with the significant relationships with performance improvement strongly support the SMA, PO, thalamus, and striatum as key regions involved in sequence-specific learning.

**FIGURE 4** Correlations: Significant negative relationships between D5 HE and SYN decreases were observed in left SMA (first row, left [$r = 0.63$, $p = .01$]), left PO (first row, right [$r = 0.63$, $p = .01$]), left thalamus (second row, left [$r = 0.53$, $p = .03$]), right thalamus (second row, right [$r = 0.54$, $p$fdr$ = .03$]) and right striatum (third row, left [$r = 0.56$, $p = .03$]). D5 HE values showed no correlation with overall performance decrease in SYN in the left premotor cortex (third row, right), left M1 (fourth row, left), and left cerebellar lobule H VI/Crus I(fourth row, right). The shaded areas around the linear slopes represent the confidence interval.

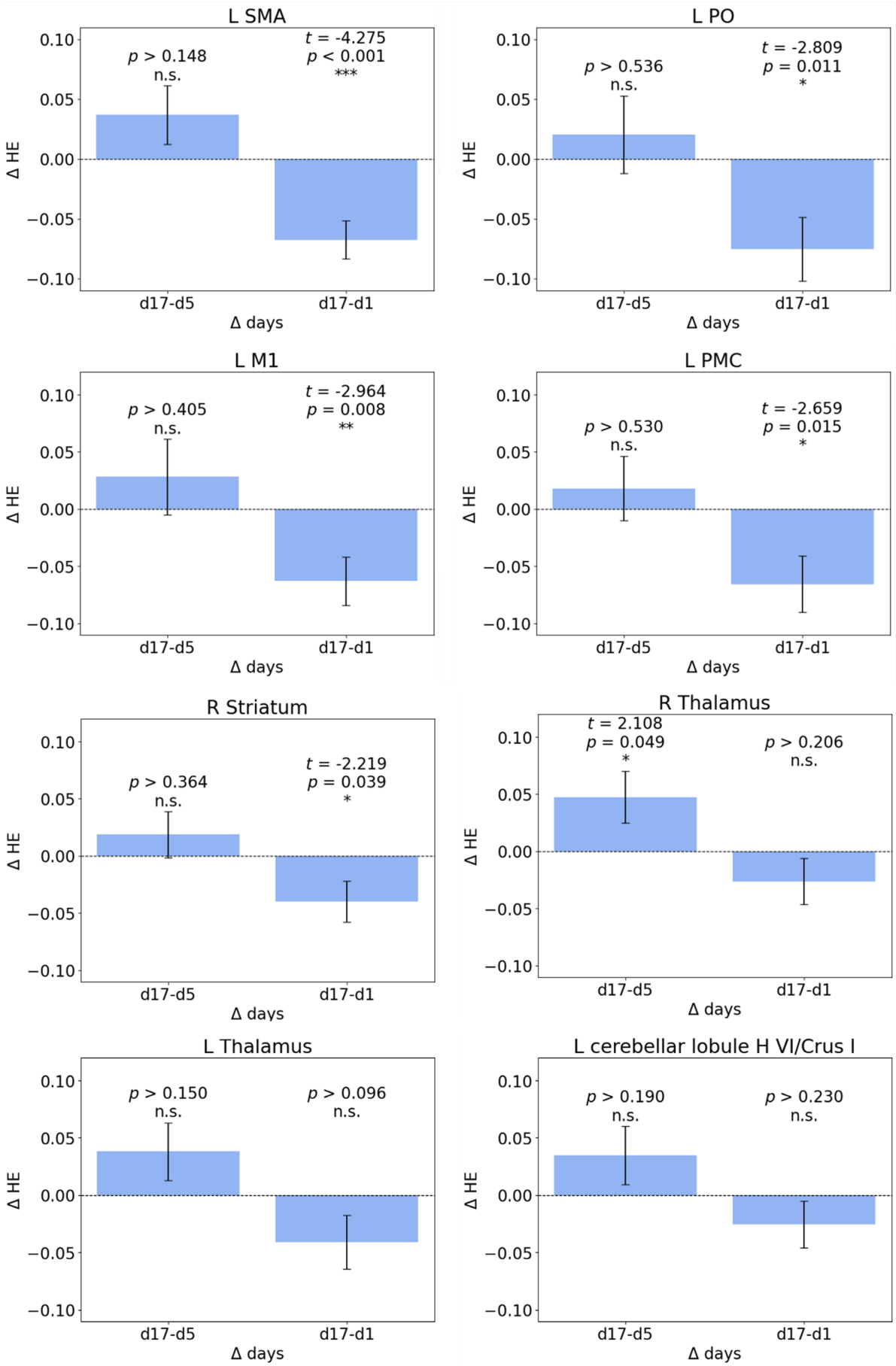


**FIGURE 5** Legend on next page.

Our previous study (Jäger et al., 2022) found the right SMA to be relevant for sequence-specific learning using EC, as supported by structural data from the same cohort (Tremblay et al., 2021). The current results showed HE decreases in left SMA with the identified cluster spanning across both hemispheres, extending our findings to this region, which has been found relevant for right-hand tasks in prior studies. HE was found to be more sensitive than EC in detecting sequence-specific changes. While the use of EC uncovered a notable sequence-specific effect within a single cluster during an interaction analysis, the majority of identified clusters displayed more pronounced changes in the control group, thus not meeting the criteria for being labeled as sequence-specific. In contrast, the HE analysis predominantly featured results influenced by the learning group, leading to their classification as a sequence- and, therefore, learning-specific. This suggests that HE might be a better measure for investigating functional neuroplastic changes following learning. Some first evidence also suggests, that HE might be less susceptible to the influence of venous biases (Huck et al., 2023). The high agreement between our results and the MSL literature supports the hypothesis that decreases in LRTC reflect cognitive function and neuroplasticity.

## 6.2 | Understanding HE changes in the context of plasticity and learning

Our findings have two main implications for neuroplasticity research. First, decreased LRTC in the resting state can indicate learning. This is consistent with previous research showing that lower LRTC of brain signals reflects cognitive effort (Barnes et al., 2009; Churchill et al., 2014, 2016; He, 2011; Kardan et al., 2020). Our study extends these findings by showing that this effect persists even while the task is not being performed. Interestingly, LRTC increased in many of the ROI's in the control group who only performed the simple sequence task and experienced no detectable behavioral improvement. We hypothesize that this increase reflects the release from effortful learning as a result of automatization and neural efficiency – providing additional support for the idea that LRTC can be used as an index of relative cognitive effort and learning. Second, posttask HE values were negatively correlated with preceding performance enhancements suggesting that behavioral improvements are also reflected in LRTC and the timing (i.e., decreased LRTC after performance improvement) indicates that it is a plastic change in response to training (Wink et al., 2006). To our knowledge, our study is the first to show decreases in LRTC outside of the active training context and during rest, which in the context of our controlled design can be interpreted as an indicator of learning.

Interestingly, previous work has linked increased LRTC with better behavioral performance (Mahjoory et al., 2019; Samek et al., 2016; Wink et al., 2006) and, similarly, Tagliazucchi et al. (2013) proposed that their observed decrease in long-range temporal memory during non-rapid eye movement (non-REM) sleep was the result of decreased conscious awareness. Our findings, which reveal decreased LRTC as a consequence of learning during the resting-state, may initially appear at odds with these studies – as they suggest that greater LRTC during rest benefits complex neural information processing and cognitive processes. However, these studies did not include a tightly matched control group nor utilize ROIS that were selected to be specific for the behavioral task for their analyses (but instead used large networks/areas and whole brain correlations). Taken together with our findings of increased LRTC in the control group, we hypothesize that increased LRTC may be a general indicator of overall performance/cognitive flexibility, whereas decreased LRTC is a specific indicator of ongoing plasticity in regions that are actively engaged in processing new information. Furthermore, given the key importance of sleep in motor learning consolidation (Vahdat et al., 2017), it is plausible that decreased LRTC during non-REM sleep and the wakeful resting-state both reflect the ongoing learning process and consolidation. As such, gaining further insights into these questions through future research would be highly valuable. An intriguing question raised by our findings is how to understand the meaning of decreases in temporal self-similarity after learning. Although we currently lack a complete understanding of the exact mechanisms involved, various neuroscientific theories shed light on potential explanations for the observed phenomenon. We can think of lower HE as indicating greater complexity and variability in the signals over time, essentially as increased noise in the signal, as opposed to higher similarity, which corresponds to more consistent, stable, and repetitive signal. Increased signal variability and noise have been shown to be beneficial for effective brain function and learning (Garrett et al., 2013; Pinneo, 1966). For instance, research in neural network dynamics and cellular interactions suggests that networks formed in the presence of increased noise show an enhanced ability to handle disturbances. This resilience contributes to better learning, adaptability, and overall optimal function (Basalyga & Salinas, 2006; Faisal et al., 2008) and might stem from noise reducing the impact of individual nodes within the network, thus offering protection against disruptions. Another concept, known as stochastic resonance, proposes that introducing moderate noise into a learning system can aid in detecting weak signals, enhancing the learning processes. (Kitajo et al., 2003; Li et al., 2006; Lugo et al., 2008; McDonnell & Abbott, 2009; Ward et al., 2006). Specifically, stochastic facilitation, observed across computational, animal, and human research, reveals that neural processes can be

**FIGURE 5** Paired samples *t*-tests of ROI timepoints in LRN: Paired sample *t*-tests were conducted between d5/d17 and d1/d17 in all ROIs of the identified sequence-specific network. In left SMA (first row, left), left PO (first row, right), left premotor cortex (second row, left), left M1 (second row, right), and right striatum (third row, left) significant differences in mean HE were found when comparing d1 and d17 but not between d5 and d17. In the right thalamus (third row, left), a significant difference was observed between d5 and d17, but not between d1 and d17.

more effective when influenced by biologically relevant noise (McDonnell & Ward, 2011; Ward et al., 2006). Furthermore, higher signal variability also guarantees a wider dynamic range of responses, which is crucial for adaptability. Essentially, increased signal variability can enhance learning by strengthening networks, improving weak signal detection, and broadening the dynamic range—ultimately facilitating the brain's adaptability and flexibility.

Another prominent theory for how optimal signal variability is able to represent brain processing is that of criticality within neuronal networks (Beggs & Plenz, 2003; He, 2011; Linkenkaer-Hansen, 2003; Shew & Plenz, 2013; Simola et al., 2017). Brain criticality indicates that neural networks operate near a tipping point between order and disorder, allowing for flexibility and adaptation. According to the criticality hypothesis, temporal brain dynamics can be homeostatically maintained within an optimal (critical/subcritical) dynamic range that allows for maximally optimized processing, and which can be modulated by task performance.

In this light, our HE decreases from d1 to d5 reflect a perturbation away from a more critical state during sequence learning – lending support to previous studies linking decreased HE to higher processing load or sensory input (e.g., Churchill et al., 2016; Ciuciu et al., 2014; He, 2011; He et al., 2010; Linkenkaer-Hansen et al., 2004; Nikulin & Brismar, 2004). In other words, the suppression of HE may be reflective of changes in functional networks as a result of ongoing synaptic plasticity related to learning. This appears to be true for cognitive effort during tasks (Barnes et al., 2009; Churchill et al., 2014; Churchill et al., 2016; Colosio et al., 2017; He, 2011; Irrmischer et al., 2018; Wink et al., 2008) and, as our results provide evidence for, throughout the entire learning period. However, the underlying mechanisms of this phenomenon are not clear and should explicitly be addressed by future studies.

Interestingly, our results provide some initial evidence that task-related regions may continue to play a role in functional representation even after training has ceased, potentially indicating their involvement in long-term sequence representations. However, as per theories of homeostasis, these maintained changes are unlikely to be permanent (Churchill et al., 2016; Dong et al., 2018; Ma et al., 2019). Future research should investigate the persistence of these changes by exploring long-range temporal memory across different timelines. Our findings suggest that HE may potentially serve as a biomarker for neuroplasticity, providing exciting opportunities for investigations in basic science and clinical rehabilitation research.

### 6.3 | Limitations

Our study offers valuable preliminary insights into the temporal dynamics underlying MSL. However, it is important to acknowledge certain limitations that may impact the interpretation of our findings. Firstly, the relatively small sample sizes in both the group undergoing MSL and the control group may affect the statistical power of our analyses, making it challenging to detect small or moderate effect sizes. Caution should be exercised when generalizing the results to larger populations, and future studies with larger sample sizes are needed to validate and replicate our findings. Secondly, a significant portion of our analyses were exploratory in nature, driven by the novelty of investigating the HE as a marker of plasticity in MSL. While these exploratory analyses can provide valuable hypotheses and insights for the future, they may also suffer from an increased risk of false positives and the potential for spurious findings. Therefore, our findings should be considered preliminary and form the basis for targeted hypotheses for future work.

## 7 | CONCLUSION

Our findings tentatively suggest that decreased LRTC in BOLD rsfMRI time series indicates functional plasticity after learning, with SMA, PO, striatum, and thalamus playing a critical role in sequence-specific motor learning.

We provide evidence to suggest that HE could be considered as a potentially sensitive regional indicator of learning that is linked to behavioral improvement—which fits with and extends a wider body of research highlighting the importance of decreased LRTC as an indicator for cognitive effort and learning—potentially reflecting a localized and lasting move away from homeostasis as the task is mastered and performance improved. Lastly, our results offer initial insights indicating that decreased long-range temporal memory resulting from learning may persist for at least 2 weeks after the conclusion of training.

### ACKNOWLEDGEMENTS

This work was supported by the Max Planck Society, the MaxNetAging Research School (Max Planck Institute for Demographic Research, ATJ), the NWO Vici grant (PI: Birte Forstmann) (PLB), the Heart and Stroke Foundation of Canada (CJS, CJG), the Michal and Renata Hornstein Chair in Cardiovascular Imaging (CJG), the National Science and Engineering Research Council (CJS: RGPIN-2020-06812; CJG: RGPIN 2015-04665) and the Fonds Recherche Québécois Nature et Technologies (CJS). Open Access funding enabled and organized by Projekt DEAL.

### CONFLICT OF INTEREST STATEMENT

The authors declare no competing financial interests.

### DATA AVAILABILITY STATEMENT

The data that support the findings of this study are available from the corresponding author upon reasonable request.

### ORCID

*Anna-Thekla P. Jäger* https://orcid.org/0000-0002-3381-8453
*Alexander Bailey* https://orcid.org/0000-0002-5586-6923
*Julia M. Huntenburg* https://orcid.org/0000-0003-0579-9811
*Christine L. Tardif* https://orcid.org/0000-0001-8356-6808
*Arno Villringer* https://orcid.org/0000-0003-2604-2404
*Claudine J. Gauthier* https://orcid.org/0000-0002-5137-5019

*Vadim Nikulin* https://orcid.org/0000-0001-6082-3859
*Pierre-Louis Bazin* https://orcid.org/0000-0002-0141-5510
*Christopher J. Steele* https://orcid.org/0000-0003-1656-7928

## REFERENCES

Abraham, A., Pedregosa, F., Eickenberg, M., Gervais, P., Mueller, A., Kossaifi, J., Gramfort, A., Thirion, B., & Varoquaux, G. (2014). Machine learning for neuroimaging with scikit-learn. *Frontiers in Neuroinformatics*, *8*, 14. https://doi.org/10.3389/fninf.2014.00014

Avants, B. B., Tustison, N., & Song, G. (2009). Advanced normalization tools (ANTS). *Insight j*, *2*, 1–35.

Barnes, A., Bullmore, E. T., & Suckling, J. (2009). Endogenous human brain dynamics recover slowly following cognitive effort. *PLoS One*, *4*(8), e6626. https://doi.org/10.1371/journal.pone.0006626

Basalyga, G., & Salinas, E. (2006). When response variability increases neural network robustness to synaptic noise. *Neural Computation*, *18*(6), 1349–1379. https://doi.org/10.1162/neco.2006.18.6.1349

Bazin, P.-L., Weiss, M., Dinse, J., Schäfer, A., Trampel, R., & Turner, R. (2014). A computational framework for ultra-high resolution cortical segmentation at 7 Tesla. *NeuroImage*, *93*(Pt 2), 201–209. https://doi.org/10.1016/j.neuroimage.2013.03.077

Beggs, J. M., & Plenz, D. (2003). Neuronal avalanches in neocortical circuits. *Journal of Neuroscience*, *23*(35), 11167–11177. https://doi.org/10.1523/JNEUROSCI.23-35-11167.2003

Berlot, E., Popp, N. J., & Diedrichsen, J. (2020). A critical re-evaluation of FMRI signatures of motor sequence learning. *ELife*, *9*, e55241. https://doi.org/10.1101/2020.01.08.899229

Bernard, J. A., & Seidler, R. D. (2013). Cerebellar contributions to visuomotor adaptation and motor sequence learning: An ALE meta-analysis. *Frontiers in Human Neuroscience*, *7*, 27. https://doi.org/10.3389/fnhum.2013.00027

Campbell, O. L., & Weber, A. M. (2022). Monofractal analysis of functional magnetic resonance imaging: An introductory review. *Human Brain Mapping*, *43*(8), 2693–2706. https://doi.org/10.1002/hbm.25801

Churchill, N. W., Cimprich, B., Askren, M. K., Reuter-Lorenz, P. A., Jung, M. S., Peltier, S., & Berman, M. G. (2014). Scale free brain dynamics under physical and psychological distress: Pre treatment effects in women diagnosed with breast cancer. *Human Brain Mapping*, *36*(3), 1077–1092. https://doi.org/10.1002/hbm.22687

Churchill, N. W., Spring, R., Grady, C., Cimprich, B., Askren, M. K., Reuter-Lorenz, P. A., Jung, M. S., Peltier, S., Strother, S. C., & Berman, M. G. (2016). The suppression of scale-free FMRI brain dynamics across three different sources of effort: Aging, task novelty and task difficulty. *Scientific Reports*, *6*(1), 30895. https://doi.org/10.1038/srep30895

Ciuciu, P., Abry, P., & He, B. J. (2014). Interplay between functional connectivity and scale-free dynamics in intrinsic FMRI networks. *NeuroImage*, *95*, 248–263. https://doi.org/10.1016/j.neuroimage.2014.03.047

Colosio, M., Shestakova, A., Nikulin, V. V., Blagovechtchenski, E., & Klucharev, V. (2017). Neural mechanisms of cognitive dissonance (revised): An EEG study. *Journal of Neuroscience*, *37*(20), 5074–5083. https://doi.org/10.1523/JNEUROSCI.3209-16.2017

Dayan, E., & Cohen, L. G. (2011). Neuroplasticity subserving motor skill learning. *Neuron*, *72*(3), 443–454. https://doi.org/10.1016/j.neuron.2011.10.008

Dong, J., Jing, B., Ma, X., Liu, H., Mo, X., & Li, H. (2018). Hurst exponent analysis of resting-state FMRI signal complexity across the adult lifespan. *Frontiers in Neuroscience*, *12*, 34. https://doi.org/10.3389/fnins.2018.00034

Eke, A., Herman, P., Sanganahalli, B. G., Hyder, F., Mukli, P., & Nagy, Z. (2012). Pitfalls in fractal time series analysis: FMRI BOLD as an exemplary case. *Frontiers in Physiology*, *3*, 32880. https://doi.org/10.3389/fphys.2012.00417

Elsinger, C. L., Harrington, D. L., & Rao, S. M. (2006). From preparation to online control: Reappraisal of neural circuitry mediating internally generated and externally guided actions. *NeuroImage*, *31*(3), 1177–1187. https://doi.org/10.1016/j.neuroimage.2006.01.041

Faisal, A., Selen, L. P., & Wolpert, D. M. (2008). Noise in the nervous system. *Nature Reviews Neuroscience*, *9*(4), 292–303. https://doi.org/10.1038/nrn2258

Floyer-Lea, A., & Matthews, P. M. (2005). Distinguishable brain activation networks for short- and long-term motor skill learning. *Journal of Neurophysiology*, *94*(1), 512–518. https://doi.org/10.1152/jn.00717.2004

Friston, K. J., Holmes, A. P., Worsley, K. J., Poline, J. P., Frith, C. D., & Frackowiak, R. S. (1994). Statistical parametric maps in functional imaging: A general linear approach. *Human Brain Mapping*, *2*(4), 189–210.

Garrett, D. D., Samanez-Larkin, G. R., MacDonald, S. W. S., Lindenberger, U., McIntosh, A. R., & Grady, C. L. (2013). Moment-to-moment brain signal variability: A next frontier in human brain mapping? *Neuroscience & Biobehavioral Reviews*, *37*(4), 610–624. https://doi.org/10.1016/j.neubiorev.2013.02.015

Gaymard, B., Pierrot-Deseilligny, C., & Rivaud, S. (1990). Impairment of sequences of memory-guided saccades after supplementary motor area lesions. *Annals of Neurology*, *28*(5), 622–626. https://doi.org/10.1002/ana.410280504

Gerloff, C., Corwell, B., Chen, R., Hallett, M., & Cohen, L. G. (1997). Stimulation over the human supplementary motor area interferes with the organization of future elements in complex motor sequences. *Brain: A Journal of Neurology*, *120*(Pt 9), 1587–1602. https://doi.org/10.1093/brain/120.9.1587

Gorgolewski, K., Burns, C.D., Madison, C., Clark, D., Halchenko, Y.O., Waskom, M.L. and Ghosh, S.S. Nipype: A flexible, lightweight and extensible neuroimaging data processing framework in python. 0.12.0-Rc1. Zenodo, 2016, https://doi.org/10.5281/zenodo.50186.

Grafton, S. T., Hazeltine, E., & Ivry, R. B. (2002). Motor sequence learning with the nondominant left hand. *Experimental Brain Research*, *146*(3), 369–378. https://doi.org/10.1007/s00221-002-1181-y

Gryga, M., Taubert, M., Dukart, J., Vollmann, H., Conde, V., Sehm, B., Villringer, A., & Ragert, P. (2012). Bidirectional gray matter changes after complex motor skill learning. *Frontiers in Systems Neuroscience*, *6*, 37. https://doi.org/10.3389/fnsys.2012.00037

Hardstone, R., Poil, S.-S., Schiavone, G., Jansen, R., Nikulin, V. V., Mansvelder, H. D., & Linkenkaer-Hansen, K. (2012). Detrended fluctuation analysis: A scale-free view on neuronal oscillations. *Frontiers in Physiology*, *3*, 450. https://doi.org/10.3389/fphys.2012.00450

Hardwick, R. M., Rottschy, C., Miall, R. C., & Eickhoff, S. B. (2013). A quantitative meta-analysis and review of motor learning in the human brain. *NeuroImage*, *67*, 283–297. https://doi.org/10.1016/j.neuroimage.2012.11.020

He, B. J. (2011). Scale-free properties of the functional magnetic resonance imaging signal during rest and task. *Journal of Neuroscience*, *31*(39), 13786–13795. https://doi.org/10.1523/JNEUROSCI.2111-11.2011

He, B. J., Zempel, J. M., Snyder, A. Z., & Raichle, M. E. (2010). The temporal structures and functional significance of scale-free brain activity. *Neuron*, *66*(3), 353–369. https://doi.org/10.1016/j.neuron.2010.04.020

Hikosaka, O., Nakahara, H., Rand, M. K., Sakai, K., Lu, X., Nakamura, K., Miyachi, S., & Doya, K. (1999). Parallel neural networks for learning sequential procedures. *Trends in Neurosciences*, *22*(10), 464–471.

Honda, M., Deiber, M. P., Ibáñez, V., Pascual-Leone, A., Zhuang, P., & Hallett, M. (1998). Dynamic cortical involvement in implicit and explicit motor sequence learning. A PET study. *Brain*, *121*(11), 2159–2173. https://doi.org/10.1093/brain/121.11.2159

Huck, J., Jäger, A.-T., Schneider, U., Grahl, S., Fan, A. P., Tardif, C., Villringer, A., Bazin, P.-L., Steele, C. J., & Gauthier, C. J. (2023). Modeling venous bias in resting state functional MRI metrics. *Human Brain Mapping*, *44*(14), 4938–4955. https://doi.org/10.1002/hbm.26431

Hunter, J. D. (2007). Matplotlib: A 2D graphics environment. *Computing in Science & Engineering*, *9*(3), 90–95.

Irrmischer, M., Poil, S.-S., Mansvelder, H. D., Intra, F. S., & Linkenkaer-Hansen, K. (2018). Strong long-range temporal correlations of beta/gamma oscillations are associated with poor sustained visual attention performance. *European Journal of Neuroscience*, *48*(8), 2674–2683. https://doi.org/10.1111/ejn.13672

Jäger, A. T. P., Huntenburg, J. M., Tremblay, S. A., Schneider, U., Grahl, S., Huck, J., Tardif, C. L., Villringer, A., Gauthier, C. J., Bazin, P. L., & Steele, C. J. (2022). Motor sequences; Separating the sequence from the motor. A longitudinal RsfMRI study. *Brain Structure and Function*, *227*(3), 793–807. https://doi.org/10.1007/s00429-021-02412-7

Janacsek, K., Shattuck, K. F., Tagarelli, K. M., Lum, J. A. G., Turkeltaub, P. E., & Ullman, M. T. (2020). Sequence learning in the human brain: A functional neuroanatomical meta-analysis of serial reaction time studies. *NeuroImage*, *207*, 116387. https://doi.org/10.1016/j.neuroimage.2019.116387

Jenkins, I. H., Brooks, D. J., Nixon, P. D., Frackowiak, R. S., & Passingham, R. E. (1994). Motor sequence learning: A study with positron emission tomography. *The Journal of Neuroscience*, *14*(6), 3775–3790. https://doi.org/10.1523/JNEUROSCI.14-06-03775.1994

Jenkinson, M. (2004). Improving the registration of B0-disorted EPI images using calculated cost function weights. Paper presented at Tenth International Conference on Functional Mapping of the Human Brain, Budapest, Hungary.

Jenkinson, M., Beckmann, C. F., Behrens, T. E. J., Woolrich, M. W., & Smith, S. M. (2012). FSL. *NeuroImage*, *62*(2), 782–790. https://doi.org/10.1016/j.neuroimage.2011.09.015

Kami, A., Meyer, G., Jezzard, P., Adams, M. M., Turner, R., & Ungerleider, L. G. (1995). Functional MRI evidence for adult motor cortex plasticity during motor skill learning. *Nature*, *377*(6545), 155–158. https://doi.org/10.1038/377155a0

Kardan, O., Adam, K. C. S., Mance, I., Churchill, N. W., Vogel, E. K., & Berman, M. G. (2020). Distinguishing cognitive effort and working memory load using scale-invariance and alpha suppression in EEG. *NeuroImage*, *211*, 116622. https://doi.org/10.1016/j.neuroimage.2020.116622

Karni, A., Meyer, G., Rey-Hipolito, C., Jezzard, P., Adams, M. M., Turner, R., & Ungerleider, L. G. (1998). The acquisition of skilled motor performance: Fast and slow experience-driven changes in primary motor cortex. *Proceedings of the National Academy of Sciences*, *95*(3), 861–868. https://doi.org/10.1073/pnas.95.3.861

Kawai, R., Markman, T., Poddar, R., Ko, R., Fantana, A. L., Dhawale, A. K., Kampff, A. R., & Ölveczky, B. P. (2015). Motor cortex is required for learning but not for executing a motor skill. *Neuron*, *86*(3), 800–812. https://doi.org/10.1016/j.neuron.2015.03.024

Kincses, Z. T., Johansen-Berg, H., Tomassini, V., Bosnell, R., Matthews, P. M., & Beckmann, C. F. (2008). Model-free characterization of brain functional networks for motor sequence learning using FMRI. *NeuroImage*, *39*(4), 1950–1958. https://doi.org/10.1016/j.neuroimage.2007.09.070

Kitajo, K., Nozaki, D., Ward, L. M., & Yamamoto, Y. (2003). Behavioral stochastic resonance within the human brain. *Physical Review Letters*, *90*(21), 218103. https://doi.org/10.1103/PhysRevLett.90.218103

Kornysheva, K., & Diedrichsen, J. (2014). Human premotor areas parse sequences into their spatial and temporal features. *eLife*, *3*, e03043. https://doi.org/10.7554/eLife.03043

Krakauer, J. W., Hadjiosif, A. M., Xu, J., Wong, A. L., & Haith, A. M. (2019). Motor learning. *Comprehensive Physiology*, *9*(2), 613–663. https://doi.org/10.1002/cphy.c170043

Lee, D., & Quessy, S. (2003). Activity in the supplementary motor area related to learning and performance during a sequential visuomotor task. *Journal of Neurophysiology*, *89*(2), 1039–1056. https://doi.org/10.1152/jn.00638.2002

Lehéricy, S., Benali, H., van de Moortele, P. F., Pélégrini-Issac, M., Waechter, T., Ugurbil, K., & Doyon, J. (2005). Distinct basal ganglia territories are engaged in early and advanced motor sequence learning. *Proceedings of the National Academy of Sciences of the United States of America*, *102*(35), 12566–12571. https://doi.org/10.1073/pnas.0502762102

Li, S.-C., von Oertzen, T., & Lindenberger, U. (2006). A neurocomputational model of stochastic resonance and aging. *Neurocomputing*, *69*(13), 1553–1560. https://doi.org/10.1016/j.neucom.2005.06.015

Linkenkaer-Hansen, K. (2003). Scaling and criticality in large-scale neuronal activity. In G. Rangarajan & M. Ding (Eds.), *Processes with long-range correlations: Theory and applications* (pp. 324–338). Springer. https://doi.org/10.1007/3-540-44832-2_18

Linkenkaer-Hansen, K., Nikulin, V. V., Palva, J. M., Kaila, K., & Ilmoniemi, R. J. (2004). Stimulus-induced change in long-range temporal correlations and scaling behaviour of sensorimotor oscillations. *The European Journal of Neuroscience*, *19*(1), 203–211. https://doi.org/10.1111/j.1460-9568.2004.03116.x

Lugo, E., Doti, R., & Faubert, J. (2008). Ubiquitous crossmodal stochastic resonance in humans: Auditory noise facilitates tactile, visual and proprioceptive sensations. *PLoS One*, *3*(8), e2860. https://doi.org/10.1371/journal.pone.0002860

Ma, Z., Turrigiano, G. G., Wessel, R., & Hengen, K. B. (2019). Cortical circuit dynamics are homeostatically tuned to criticality in vivo. *Neuron*, *104*(4), 655–664.e4. https://doi.org/10.1016/j.neuron.2019.08.031

Mahjoory, K., Cesnaite, E., Hohlefeld, F. U., Villringer, A., & Nikulin, V. V. (2019). Power and temporal dynamics of alpha oscillations at rest differentiate cognitive performance involving sustained and phasic cognitive control. *NeuroImage*, *188*, 135–144. https://doi.org/10.1016/j.neuroimage.2018.12.001

Matsuzaka, Y., Picard, N., & Strick, P. L. (2007). Skill representation in the primary motor cortex after long-term practice. *Journal of Neurophysiology*, *97*(2), 1819–1832. https://doi.org/10.1152/jn.00784.2006

Maxim, V., Şendur, L., Fadili, J., Suckling, J., Gould, R., Howard, R., & Bullmore, E. (2005). Fractional Gaussian noise, functional MRI and Alzheimer's disease. *NeuroImage*, *25*(1), 141–158. https://doi.org/10.1016/j.neuroimage.2004.10.044

McDonnell, M. D., & Ward, L. M. (2011). The benefits of noise in neural systems: Bridging theory and experiment. *Nature Reviews Neuroscience*, *12*(7), 415–426. https://doi.org/10.1038/nrn3061

McDonnell, M. D., & Abbott, D. (2009). What is stochastic resonance? Definitions, misconceptions, debates, and its relevance to biology. *PLoS Computational Biology*, *5*(5), e1000348. https://doi.org/10.1371/journal.pcbi.1000348

McIntosh, A. R., Kovacevic, N., Lippe, S., Garrett, D., Grady, C., & Jirsa, V. (2010). The development of a noisy brain. *Archives Italiennes de Biologie*, *148*(3), 323–337.

Mushiake, H., Inase, M., & Tanji, J. (1991). Neuronal activity in the primate premotor, supplementary, and precentral motor cortex during visually guided and internally determined sequential movements. *Journal of Neurophysiology*, *66*(3), 705–718. https://doi.org/10.1152/jn.1991.66.3.705

Neudorf, J., Ekstrand, C., Kress, S., & Borowsky, R. (2020). Brain structural connectivity predicts brain functional complexity: diffusion tensor imaging derived centrality accounts for variance in fractal properties of functional magnetic resonance imaging signal. *Neuroscience*, *438*, 1–8. https://doi.org/10.1016/j.neuroscience.2020.04.048

Nikulin, V. V., & Brismar, T. (2004). Long-range temporal correlations in alpha and beta oscillations: Effect of arousal level and test–retest reliability. *Clinical Neurophysiology*, *115*(8), 1896–1908. https://doi.org/10.1016/j.clinph.2004.03.019

Pedregosa, F., Varoquaux, G., Gramfort, A., Michel, V., Thirion, B., Grisel, O., … Duchesnay, E. (2011). Scikit-learn: Machine learning in Python. *The Journal of Machine Learning research*, *12*, 2825–2830.

Penhune, V. B., & Doyon, J. (2002). Dynamic cortical and subcortical networks in learning and delayed recall of timed motor sequences. *Journal of Neuroscience*, *22*(4), 1397–1406. https://doi.org/10.1523/JNEUROSCI.22-04-01397.2002

Penhune, V. B., & Steele, C. J. (2012). Parallel contributions of cerebellar, striatal and M1 mechanisms to motor sequence learning. *Behavioural Brain Research*, *226*(2), 579–591. https://doi.org/10.1016/j.bbr.2011.09.044

Picard, N., Matsuzaka, Y., & Strick, P. L. (2013). Extended practice of a motor skill is associated with reduced metabolic activity in M1. *Nature Neuroscience*, *16*(9), 1340–1347. https://doi.org/10.1038/nn.3477

Pinneo, L. R. (1966). On noise in the nervous system. *Psychological Review*, *73*, 242–247. https://doi.org/10.1037/h0023240

Poldrack, R. A., Mumford, J. A., & Nichols, T. E. (2011). *Handbook of functional MRI data analysis*. Cambridge University Press.

Power, J. D., Barnes, K. A., Snyder, A. Z., Schlaggar, B. L., & Petersen, S. E. (2012). Spurious but systematic correlations in functional connectivity MRI networks arise from subject motion. *NeuroImage*, *59*(3), 2142–2154. https://doi.org/10.1016/j.neuroimage.2011.10.018

R Core Team. (2021). *R: A language and environment for statistical computing*. R Foundation for Statistical Computing. https://www.R-project.org/

Reithler, J., van Mier, H. I., & Goebel, R. (2010). Continuous motor sequence learning: Cortical efficiency gains accompanied by striatal functional reorganization. *NeuroImage*, *52*(1), 263–276. https://doi.org/10.1016/j.neuroimage.2010.03.073

Roche, A. (2011). A four-dimensional registration algorithm with application to joint correction of motion and slice timing in FMRI. *IEEE Transactions on Medical Imaging*, *30*(8), 1546–1554. https://doi.org/10.1109/TMI.2011.2131152

Samek, W., Blythe, D. A. J., Curio, G., Müller, K.-R., Blankertz, B., & Nikulin, V. V. (2016). Multiscale temporal neural dynamics predict performance in a complex sensorimotor task. *NeuroImage*, *141*, 291–303. https://doi.org/10.1016/j.neuroimage.2016.06.056

Schaworonkow, N., Blythe, D. A. J., Kegeles, J., Curio, G., & Nikulin, V. V. (2015). Power-law dynamics in neuronal and behavioral data introduce spurious correlations. *Human Brain Mapping*, *36*(8), 2901–2914. https://doi.org/10.1002/hbm.22816

Shew, W. L., & Plenz, D. (2013). The functional benefits of criticality in the cortex. *The Neuroscientist*, *19*(1), 88–100. https://doi.org/10.1177/1073858412445487

Shibasaki, H., Sadato, N., Lyshkow, H., Yonekura, Y., Honda, M., Nagamine, T., Suwazono, S., Magata, Y., Ikeda, A., Miyazaki, M., Fukuyama, H., Asato, R., & Konishi, J. (1993). Both primary motor cortex and supplementary motor area play an important role in complex finger movement. *Brain*, *116*(6), 1387–1398. https://doi.org/10.1093/brain/116.6.1387

Shima, K., & Tanji, J. (2000). Neuronal activity in the supplementary and presupplementary motor areas for temporal organization of multiple movements. *Journal of Neurophysiology*, *84*(4), 2148–2160. https://doi.org/10.1152/jn.2000.84.4.2148

Simola, J., Zhigalov, A., Morales-Muñoz, I., Palva, J. M., & Palva, S. (2017). Critical dynamics of endogenous fluctuations predict cognitive flexibility in the Go/NoGo task. *Scientific Reports*, *7*(1), 2909. https://doi.org/10.1038/s41598-017-02750-9

Sokunbi, M. O., Gradin, V. B., Waiter, G. D., Cameron, G. G., Ahearn, T. S., Murray, A. D., Steele, D. J., & Staff, R. T. (2014). Nonlinear complexity analysis of brain FMRI signals in schizophrenia. *PLoS One*, *9*(5), e95146. https://doi.org/10.1371/journal.pone.0095146

Steele, C. J., & Penhune, V. B. (2010). Specific increases within global decreases: A functional magnetic resonance imaging investigation of five days of motor sequence learning. *Journal of Neuroscience*, *30*(24), 8332–8341. https://doi.org/10.1523/JNEUROSCI.5569-09.2010

Suckling, J., Wink, A. M., Bernard, F. A., Barnes, A., & Bullmore, E. (2008). Endogenous multifractal brain dynamics are modulated by age, cholinergic blockade and cognitive performance. *Journal of Neuroscience Methods*, *174*(2), 292–300. https://doi.org/10.1016/j.jneumeth.2008.06.037

Tagliazucchi, E., Wegner, F. von, Morzelewski, A., Brodbeck, V., Jahnke, K., & Laufs, H. (2013). Breakdown of long-range temporal dependence in default mode and attention networks during deep sleep. *Proceedings of the National Academy of Sciences*, *110*(38), 15419–15424. https://doi.org/10.1073/pnas.1312848110

Tanaka, S., Honda, M., Hanakawa, T., & Cohen, L. G. (2010). Differential contribution of the supplementary motor area to stabilization of a procedural motor skill acquired through different practice schedules. *Cerebral Cortex (New York, NY)*, *20*(9), 2114–2121. https://doi.org/10.1093/cercor/bhp276

Tanji, J., & Shima, K. (1994). Role for supplementary motor area cells in planning several movements ahead. *Nature*, *371*(6496), 413–416. https://doi.org/10.1038/371413a0

Tetereva, A., Kartashov, S., Ivanitsky, A., & Martynova, O. (2020). Variance and scale-free properties of resting-state blood oxygenation level-dependent signal after fear memory acquisition and extinction. *Frontiers in Human Neuroscience*, *14*, 509075. https://doi.org/10.3389/fnhum.2020.509075

Tognoli, E., & Scott Kelso, J. A. (2014). The Metastable Brain. *Neuron*, *81*(1), 35–48. https://doi.org/10.1016/j.neuron.2013.12.022

Tremblay, S. A., Jäger, A.-T., Huck, J., Giacosa, C., Beram, S., Schneider, U., Grahl, S., Villringer, A., Tardif, C. L., Bazin, P.-L., Steele, C. J., & Gauthier, C. J. (2021). White matter microstructural changes in short-term learning of a continuous visuomotor sequence. *Brain Structure and Function*, *226*(6), 1677–1698. https://doi.org/10.1007/s00429-021-02267-y

Vahdat, S., Fogel, S., Benali, H., & Doyon, J. (2017). Network-wide reorganization of procedural memory during NREM sleep revealed by FMRI. *ELife*, *6*, e24987. https://doi.org/10.7554/eLife.24987

Virtanen, P., Gommers, R., Oliphant, T. E., Haberland, M., Reddy, T., Cournapeau, D., Burovski, E., Peterson, P., Weckesser, W., Bright, J., van der Walt, S. J., Brett, M., Wilson, J., Millman, K. J., Mayorov, N., Nelson, A. R. J., Jones, E., Kern, R., Larson, E., … Vázquez-Baeza, Y. (2020). SciPy 1.0: Fundamental algorithms for scientific computing in python. *Nature Methods*, *17*(3), 261–272. https://doi.org/10.1038/s41592-019-0686-2

Vollmann, H., Conde, V., Sewerin, S., Taubert, M., Sehm, B., Witte, O. W., Villringer, A., & Ragert, P. (2013). Anodal transcranial direct current stimulation (TDCS) over supplementary motor area (SMA) but not pre-SMA promotes short-term visuomotor learning. *Brain Stimulation*, *6*(2), 101–107. https://doi.org/10.1016/j.brs.2012.03.018

Ward, L. M., Doesburg, S. M., Kitajo, K., MacLean, S. E., & Roggeveen, A. B. (2006). Neural synchrony in stochastic resonance, attention, and consciousness. *Canadian Journal of Experimental Psychology*, *60*(4), 319–326. https://doi.org/10.1037/cjep2006029

Waskom, M. L. (2021). Seaborn: Statistical data visualization. *Journal of Open Source Software*, *6*(60), 3021.

Wei, M., Qin, J., Yan, R., Li, H., Yao, Z., & Lu, Q. (2013). Identifying major depressive disorder using hurst exponent of resting-state brain networks. *Psychiatry Research: Neuroimaging*, *214*(3), 306–312. https://doi.org/10.1016/j.pscychresns.2013.09.008

Wenger, E., Brozzoli, C., Lindenberger, U., & Lövdén, M. (2017). Expansion & renormalization of human brain structure during skill acquisition. *Trends in Cognitive Sciences*, *21*(12), 930–939. https://doi.org/10.1016/j.tics.2017.09.008

Wiestler, T., & Diedrichsen, J. (2013). Skill learning strengthens cortical representations of motor sequences. *eLife*, *2*, e00801. https://doi.org/10.7554/eLife.00801

Wink, A. M., Bernard, F., Salvador, R., Bullmore, E., & Suckling, J. (2006). Age and cholinergic effects on hemodynamics and functional coherence of human hippocampus. *Neurobiology of Aging*, *27*(10), 1395–1404. https://doi.org/10.1016/j.neurobiolaging.2005.08.011

Wink, A.-M., Bullmore, E., Barnes, A., Bernard, F., & Suckling, J. (2008). Monofractal and multifractal dynamics of low frequency endogenous brain oscillations in functional MRI. *Human Brain Mapping*, *29*(7), 791–801. https://doi.org/10.1002/hbm.20593

Woo, C.-W., Krishnan, A., & Wager, T. D. (2014). Cluster-extent based thresholding in FMRI analyses: Pitfalls and recommendations. *NeuroImage*, *91*, 412–419. https://doi.org/10.1016/j.neuroimage.2013.12.058

Wu, J., Srinivasan, R., Kaur, A., & Cramer, S. C. (2014). Resting-state cortical connectivity predicts motor skill acquisition. *NeuroImage*, *91*, 84–90. https://doi.org/10.1016/j.neuroimage.2014.01.026

Yokoi, A., Arbuckle, S. A., & Diedrichsen, J. (2018). The role of human primary motor cortex in the production of skilled finger sequences. *The Journal of Neuroscience*, *38*(6), 1430–1442. https://doi.org/10.1523/JNEUROSCI.2798-17.2017

Yokoi, A., & Diedrichsen, J. (2019). Neural organization of hierarchical motor sequence representations in the human neocortex. *Neuron*, *103*, 1178–1190.e7. https://doi.org/10.1016/j.neuron.2019.06.017

## SUPPORTING INFORMATION

Additional supporting information can be found online in the Supporting Information section at the end of this article.

**How to cite this article:** Jäger, A.-T. P., Bailey, A., Huntenburg, J. M., Tardif, C. L., Villringer, A., Gauthier, C. J., Nikulin, V., Bazin, P.-L., & Steele, C. J. (2024). Decreased long-range temporal correlations in the resting-state functional magnetic resonance imaging blood-oxygen-level-dependent signal reflect motor sequence learning up to 2 weeks following training. *Human Brain Mapping*, *45*(4), e26539. https://doi.org/10.1002/hbm.26539